Molecular basis of diseases caused by the mtDNA mutation m.8969G>A in the subunit *a* of ATP synthase

Natalia Skoczeń[1,2$], Alain Dautant[2,3$], Krystyna Binko[1,2], François Godard[2,3], Marine Bouhier[2,3], Xin Su [4,5], Jean-Paul Lasserre[2,3], Marie-France Giraud[2,3], Déborah Tribouillard-Tanvier[2,3£], Huimei Chen[4], Jean-Paul di Rago[2,3]*, Roza Kucharczyk[1]*

[1]Institute of Biochemistry and Biophysics, Polish Academy of Sciences, Warsaw, Poland
[2]CNRS, Institut de Biochimie et Génétique Cellulaires, UMR 5095, F-33077 Bordeaux, France
[3]Université de Bordeaux, IBGC, UMR 5095, F-33077 Bordeaux, France
[4]Nanjing University School of Medicine, Nanjing, Jiangsu, China
[5]Center of Drug Discovery, State Key Laboratory of Natural Medicines, China Pharmaceutical University, Nanjing, Jiangsu, China
[£]Research Associate from INSERM

[$]These authors equally contributed

*Corresponding authors: roza@ibb.waw.pl or jp.dirago@ibgc.cnrs.fr

Abstract

The ATP synthase which provides aerobic eukaryotes with ATP, organizes into a membrane-extrinsic catalytic domain, where ATP is generated, and a membrane-embedded F_O domain that shuttles protons across the membrane. We previously identified a mutation in the mitochondrial *MT-ATP6* gene (m.8969G>A) in a 14-year-old Chinese female who developed an isolated nephropathy followed by brain and muscle problems. This mutation replaces a highly conserved serine residue into asparagine at amino acid position 148 of the membrane-embedded subunit *a* of ATP synthase. We showed that an equivalent of this mutation in yeast ($aS_{175}N$) prevents F_O-mediated proton translocation. Herein we identified four first-site intragenic suppressors ($aN_{175}D$, $aN_{175}K$, $aN_{175}I$, and $aN_{175}T$), which, in light of a recently published atomic structure of yeast F_O, indicating that the detrimental consequences of the original mutation result from the establishment of hydrogen bonds between aN_{175} and a nearby glutamate residue (aE_{172}) that was proposed to be critical for the exit of protons from the ATP synthase towards the mitochondrial matrix. Interestingly also, we found that the $aS_{175}N$ mutation can be suppressed by second-site suppressors ($aP_{12}S$, $aI_{171}F$, $aI_{171}N$, $aI_{239}F$, and $aI_{200}M$), of which some are very distantly located (by 20-30 Å) from the original mutation. The possibility to compensate through long-range effects the $aS_{175}N$ mutation is an interesting observation that holds promise for the development of therapeutic molecules.

Keywords: ATP synthase, subunit *a*, mtDNA, *MT-ATP6*, oxidative phosphorylation, metabolic disease

1. Introduction

The ATP synthase is found in the inner mitochondrial membrane and catalyzes the last step in oxidative phosphorylation (OXPHOS) by producing ATP from ADP and inorganic phosphate using the transmembrane proton gradient, also called the proton-motive force (*pmf*), generated during the transfer of electrons to oxygen by the respiratory chain (RC) complexes (I–IV) [1]. Cryo-EM structures of the bovine *Bos taurus* and yeasts *Yarrowia lipolytica* and *Saccharomyces cerevisiae* F_1F_O ATP synthases, that are basically of the same subunit composition and structural construction as the human enzyme, have been described recently [2-5]. The ATP synthase organizes into a membrane-extrinsic F_1 catalytic and a membrane-embedded F_O domain that are connected by a peripheral and central stalk [4, 6]. ATP synthase exists as dimers [2, 6] that assemble into long ribbons important for cristae formation [7, 8], which is crucial with respect to accommodation within the mitochondrial inner membrane of the OXPHOS respiratory chain complexes and the ATP synthase in most efficient and native way.

Within the F_O, protons are shuttled across the membrane by subunit *a* and a ring of identical subunits *c* (8 in mammals, 10 in yeast). Hydrophilic amino acids of subunit *a* allow protons to enter the F_O from the IMS. Approximately in the middle of the membrane the proton can bind to a highly conserved acidic residue of subunit *c* helix 2 (*c*H2) (cE_{59} in *H. sapiens*) located at the outer surface of the *c*-ring. The binding of a proton on this carboxylate residue disrupts a previously established electrostatic interaction of cE_{59} with a highly conserved positively charged arginine residue in subunit *a* membrane helix 5 (*a*H5) (aR_{159} in *H. sapiens*) [5, 9, 10]. This arginine acts as an electrostatic separator between the proton pathway from the IMS to the middle of the membrane and a second, spatially separated pathway that allow

incoming protons still bound on the *c*-ring glutamate to be released into the matrix [11]. The operation direction of this process is primarily driven by the ion gradient that causes a ratchet type mechanism of the neutralized *c*-ring glutamate in the hydrophobic membrane, which does energetically not allow the back stepping without externally applied force [9, 10]. After an almost complete revolution of the *c*-ring, the glutamate is deprotonated in the aqueous exit channel [12] and the proton is moved towards the mitochondrial matrix [2, 4-6, 13]. The *c*-ring is tightly bound to the central stalk, a three subunit subcomplex of F_1 ($\gamma\delta\varepsilon$), which induces upon rotation cyclic conformational changes in the $(\alpha\beta)_3$ catalytic head of F_1 that favor synthesis and release of ATP [14], according to the binding change mechanism [1].

Devastating human neuromuscular disorders (e.g. Neuropathy, Ataxia, and Retinitis Pigmentosa (NARP) and Maternally Inherited Leigh Syndrome (MILS)) have been associated to numerous mutations in subunit *a* [15]. This protein is encoded by the mitochondrial *MT-ATP6* gene. Human cells contain up to thousands copies of mtDNA [16]. Mutations in this DNA are highly recessive and usually co-exist in patient's cells and tissues with wild type mtDNA molecules, a situation referred to as heteroplasmy. These features make it difficult to precisely know how specific pathogenic mtDNA mutations influence oxidative phosphorylation. To better characterize the effects of disease-causing subunit *a* mutations, we exploited unique features of *Saccharomyces cerevisiae*. Mitochondria from this single-celled fungus and humans show many similarities [17-21], and mitochondrial genetic transformation can be achieved in this yeast in a highly controlled fashion, by the biolistic delivery into mitochondria of in-vitro-made mutated mtDNA fragments, followed by their integration into wild type mtDNA by homologous DNA recombination [22]. Being unable to stably maintain heteroplasmy [23], it is easy to obtain yeast homoplasmic

populations where all mtDNA molecules carry a mutation of interest. Owing to its good fermenting capacity, yeast models of human mitochondrial diseases can be kept alive when provided with sugars like glucose even when oxidative phosphorylation is completely inactivated [24, 25].

We used this yeast-based approach to investigate the impact on ATP synthase of nine subunit *a* missense mutations identified in patients [15, 25-33]. Some of these mutations were found to compromise incorporation of subunit *a* into ATP synthase, whereas others prevent the functioning of F_O without minor or any assembly defect. While these observations are interesting, it is often difficult to understand why the mutations are detrimental. Further information may be obtained by the isolation of intragenic suppressor mutations. In doing so, it is possible to identify novel amino acids at the original mutation site that are compatible with subunit *a* function as well as second-site suppressors that make the primary mutation no longer or less detrimental.

We here applied this suppressor genetics approach to a mutation in subunit *a* (m.8969G>A, *a*S_{148}N) that we previously identified in a 14-year-old Chinese female who initially developed an isolated nephropathy followed by a complex clinical presentation with brain and muscle problems [33]. With an equivalent of this mutation (*a*S_{175}N), yeast fails to grow on non-fermentable carbon sources due to a lack of F_O-mediated proton transfer [33]. The isolation of respiratory sufficient revertants from the mutant *a*S_{175}N led us to identify four first-site (*a*N_{175}D, *a*N_{175}K, *a*N_{175}I, and *a*N_{175}T) and five second-site (*a*P_{12}S, *a*I_{171}F, *a*I_{171}N, *a*I_{239}F, and *a*I_{200}M) suppressor mutations restoring to varying degree ATP synthase function. The results, in the light of a recently published atomic structure of yeast F_O [5, 34], indicate that the detrimental consequences of the *a*S_{175}N mutation may result from the establishment of hydrogen

122 bonds between *a*N_{175} and *a*E_{172}, a residue that was proposed to be critical for the exit
123 of protons from ATP synthase towards the mitochondrial matrix [5].
124
125
126
127

2. Materials and Methods

2.1. Growth media and genotypes

The media used for growing yeast were: YPGA (1% Bacto yeast extract, 1% Bacto Peptone, 2% or 10% glucose, 40 mg/L adenine), YPGalA (1% Bacto yeast extract, 1% Bacto Peptone, 2% galactose, 40 mg/L adenine), YPEGA (1% Bacto yeast extract, 1% Bacto Peptone, 3% ethanol, 2% glycerol, 40 mg/L adenine), W0 (2% glucose, 0.67% Nitrogen base with ammonium sulfate from Difco). SP1: 0.1% glucose, 0.25% yeast extract, 50 mM potassium acetate. Solid media were obtained by adding 2% Bacto Agar (Difco, Becton Dickinson). The genotypes of the strains used in this study are listed in Table 1. Growth curves were established with the Bioscreen C^{TM} system.

2.2. Selection of respiratory-sufficient revertants from the yeast *a*S$_{175}$N mutant

The *a*S$_{175}$N mutant (strain RKY105) was subcloned on rich 2% glucose plates. Forty single colonies were picked up and individually grown in 10% glucose. Glucose was removed from the cultures by two washings with water and 10^8 cells from each culture were spread on rich glycerol/ethanol (YPEGA) plates. The plates were incubated at 28°C for 25 days. Maximum 3 revertants per plate were retained for further analysis. The revertants were purified by subcloning on glucose plates. They were crossed on W0 minimal medium to strain D273-10B/60 devoid of mtDNA (ρ^o), and the diploid cells were tested for their ability to grow on glycerol. The *ATP6* gene was amplified by PCR with primers oATP6-1 5'TAATATACGGGGGTGGGTCCCTCAC and oATP6-10 5'GGGCCGAACTCCGAAGGAGTAAG, and sequenced entirely.

2.3. Bioenergetics analyses

153 Mitochondrial enzyme assays and membrane potential analyses were performed on
154 mitochondria isolated from yeast cells grown in rich galactose (YPGalA) at 28°C.
155 Mitochondria were prepared by the enzymatic method, as described [35]. Oxygen
156 consumption rates were measured with a Clark electrode in 0.65 M mannitol, 0.36
157 mM EGTA, 5 mM Tris/phosphate, 10 mM Tris/maleate pH 6.8 (respiration buffer), as
158 described [36]. For ATP synthesis rate measurements, the mitochondria (0.15 mg/ml)
159 were placed in a 1 ml thermostatically controlled chamber at 28°C in respiration
160 buffer. The reaction was started by adding 4 mM NADH and 750 µM ADP; 100 µl
161 aliquots were taken every 15 seconds (30 seconds for strains with a slow oxygen
162 consumption rate) and the reaction was stopped by adding 3.5% perchloric acid and
163 12.5 mM EDTA. Samples were neutralized to pH 6.5 by KOH and 0.3 M MOPS. ATP
164 was quantified using the Kinase-Glo Max Luminescence Kinase Assay (Promega)
165 and a Beckman Coulter's Paradigm Plate Reader. Part of the ATP produced by the
166 F_1F_O-ATP synthase was assessed using oligomycin (20 µg/mg of proteins).
167 Variations in transmembrane potential ($\Delta\Psi$) were evaluated in the respiration buffer
168 using Rhodamine 123 (0.5 µg/ml), with λ^{exc} of 485 nm and λ^{em} of 533 nm under
169 constant stirring with a Cary Eclipse Fluorescence Spectrophotometer (Agilent
170 Technologies, Santa Clara, CA, USA) [37].

171 2.4. BN-PAGE analyses

172 Blue native-PAGE experiments were carried out as described [38]. 200 µg of
173 mitochondrial proteins suspended in 100 µl extraction buffer (30 mM HEPES pH=6,8,
174 150 mM potassium acetate, 12% glycerol, 2 mM 6-aminocaproic acid, 1 mM EGTA,
175 1.5% digitonin (Sigma)), supplemented with one protease inhibitor cocktail tablet from
176 Roche. After 30 min incubation on ice, the extracts were cleared by centrifugation
177 (14,000 rpm, 4°C, 30 min), supplemented with 4.5 µl of loading dye (5% Serva Blue

G-250, 750 mM 6-aminocaproic acid) and run on NativePAGE^{TM} 3-12% Bis-Tris Gels (Invitrogen). After transfer onto a PVDF membrane, ATP synthase complexes were detected using polyclonal antibodies raised against α-F1 subunit (Atp1p) or subunit *a* (Atp6) of yeast ATP synthase, at 1:10000 dilution.

2.5. Amino-acid alignments and topology of subunit *a* mutations.

Multiple sequence alignment of ATP synthase *a*-subunits of various origins was performed using COBALT [39]. The topology of the mutations within F_O structure is based on the atomic structure of F_O recently published [5]. The shown figures were built using PyMOL molecular graphic system.

2.6. Statistical analysis

At least three biological and three technical replicates for performed for all experiments. The *t*-test was used for all data sets. Significance and confidence level was set at 0.05.

3. Results

Yeast subunit *a* (also referred to as subunit *6* or Atp6p) is synthesized as a pre-protein of which the first ten residues are removed during assembly [33]. The serine residue at position 148 of human subunit *a* that is changed into asparagine by the m.8969G>A mutation corresponds to aS_{175} in the non-processed yeast protein (Fig. 1). As we have shown, a yeast model of the m.8969G>A mutation ($aS_{175}N$) fails to grow on non-fermentable substrates like glycerol owing to a lack in F_O-mediated proton transport [33]. Compared to wild type (*WT*) yeast, fully assembled F_1F_O complexes accumulate slightly less in the $aS_{175}N$ mutant and free F_1 particles are detectable in BN-gels ([33], see also below). This effect may be in part or mostly due to a higher propensity of the $aS_{175}N$ mutant to produce ρ^-/ρ^0 cells issued from large deletions in mtDNA (30% vs <5% in the *WT*). A decreased mtDNA stability was observed in many other yeast mutants in which ATP synthase function is severely compromised [40]. Thus, rather than a wide impact on ATP synthase structure, the $aS_{175}N$ mutation most likely locally disturbs this structure.

3.1. Isolation of revertants from the mutant $aS_{175}N$

We isolated revertants from the $aS_{175}N$ mutant, using a previously described procedure [41]. To ensure genetic independence, they were isolated from different $aS_{175}N$ subclones grown in liquid glucose. The cells were spread on glycerol medium (10^8 cells/plate). Revertants appeared at a 10^{-7} frequency. 73 isolates were retained for analysis. After crossing with a strain (D273-10B/60) having a wild type nucleus and totally devoid of mitochondrial DNA (ρ^o), the revertants were still able to grow on glycerol indicating that the suppressor mutations were nuclear dominant or located in mitochondrial DNA. Most (>95%) of the spores from at least 6 complete tetrads issued from the diploid revertants were able to grow on glycerol (not shown)

indicating that the suppressor mutations had a mitochondrial origin, otherwise they would have displayed a mendelian (2:2) segregation. The gene *ATP6* was entirely sequenced in each revertant. In 60 revertants, a novel mutation in *ATP6* (intragenic suppressor) was identified (Table 2). Two nucleotide changes were introduced at codon 175 to replace serine by asparagine ($TCT_{175}AAT$). Not surprisingly, none of the sequenced revertants had recovered a wild type *ATP6* gene because the frequency of a specific double nucleotide change is far below 10^{-10}. However six clones had again a serine codon at position 175 that was derived from a single nucleotide change ($AAT_{175}AGT$); they all grew on glycerol like wild type yeast (not shown) and were not analyzed further. Four other first-site mutations introduced novel amino acid residues at position 175: $AAT_{175}GAT$ ($aN_{175}D$) in two clones, $AAT_{175}AAA$ ($aN_{175}K$) in one clone, $AAT_{175}ATT$ ($aN_{175}I$) in two clones, and $AAT_{175}ACT$ ($aN_{175}T$) in one clone. Henceforth, the four different pseudo first-site reversions will be designated as $aS_{175}D$ (instead of $aN_{175}D$), $aS_{175}K$, $aS_{175}I$, and $aS_{175}T$ to indicate the amino-acid changes relative to the wild type protein sequence.

In 48 revertants, respiration-dependent growth recovery resulted from a single nucleotide change in *ATP6* not located at codon 175 (second-site intragenic suppressor): $CCA_{12}TCA$ ($aP_{12}S$) in 3 clones, $ATT_{171}TTT$ ($aI_{171}F$) in 8 clones, $ATT_{171}AAT$ ($aI_{171}N$) in 1 clone, $ATT_{239}TTT$ ($aI_{239}F$) in 35 clones, and $ATT_{200}ATA$ ($aI_{200}M$) in 1 clone (Fig. 1, Table 2).

Finally, the remaining 13 revertants had no other mutation in *ATP6* than the original one, $aS_{175}N$. We considered the possibility that these revertants were issued from an extragenic suppressor in one of the two other mitochondrial ATP synthase genes, *ATP8* and *ATP9*, but no mutation was detected in these genes. These revertants were not analyzed further.

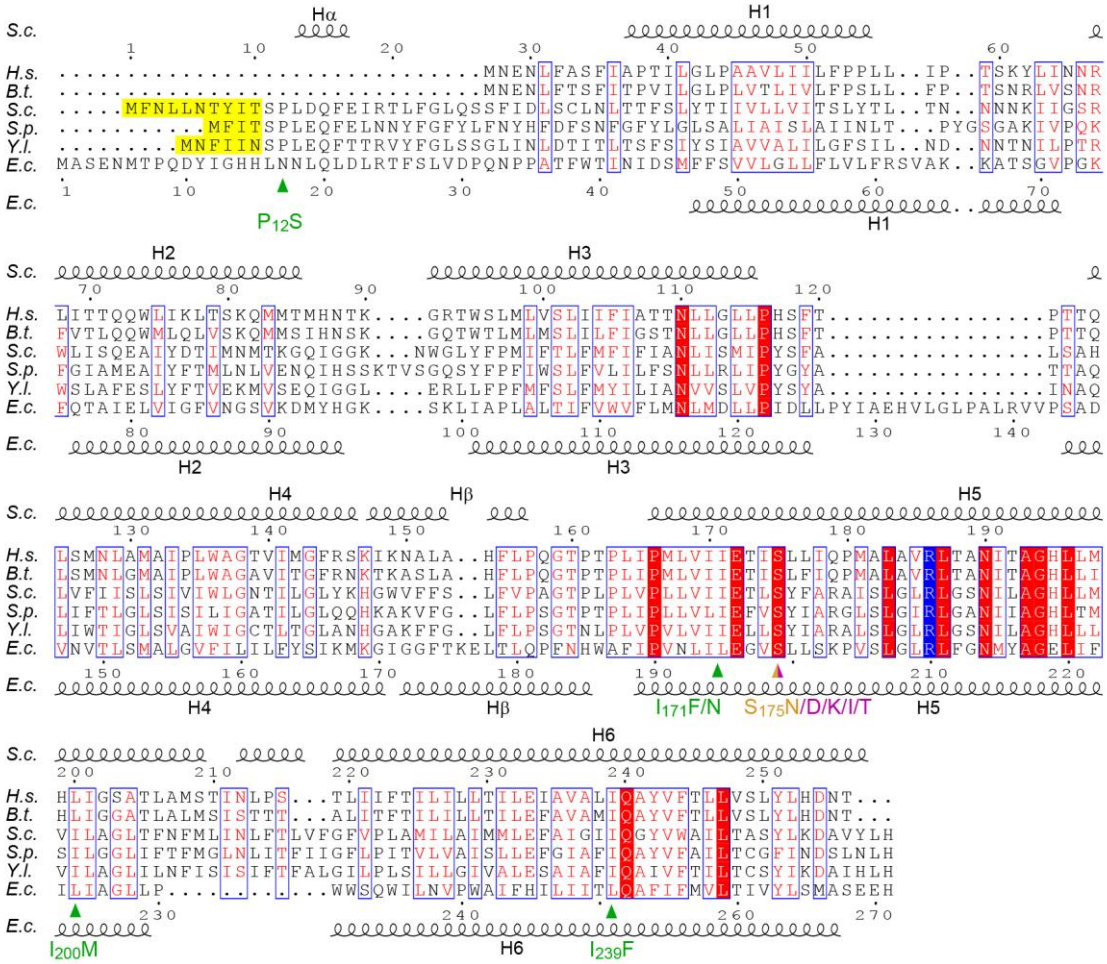

Figure 1. Sequence alignments of subunits *a* from various sources and conservation of the residues modified by the suppressors of $S_{175}N$. The aligned subunits *a* are from *Homo sapiens (H.s.), Bos taurus (B.t.), Saccharomyces cerevisiae (S.c.), Schizosaccharomyces pombe (S.p.), Yarrowia lipolytica (Y.l.) and Escherichia coli (E.c.).* The magenta and green arrows mark the locations of the pseudo first-site and the second-site intragenic mutations found in this study, respectively. The maroon arrow marks the original $S_{175}N$ mutation. At the top and bottom, the residues are numbered according to the unprocessed *S.c*. protein (the first 10 residues are cleaved during assembly of the protein [42] and to *E.c.* protein, respectively. Leader peptide sequences in the subunits *a* of *S.c*., *S.p.* and *Y.l*. [43] are marked in yellow. Strictly conserved residues are in white characters on a red background while similar residues are in red on a white background with blue frames.

α-helices in the *S.c.* and *E.c.* proteins, marked above and below amino the alignment, are according to *Y.l.* and *E.c.* structures, respectively [2, 5, 44]. The essential arginine is on a blue background.

3.2. Properties of the revertants.

3.2.1. Respiratory growth and mtDNA stability

Of the nine different intragenic suppressors we isolated from the *a*S_{175}N mutant, four (*a*S_{175}I, *a*S_{175}T, *a*I_{171}F, and I_{200}M) conferred a good growth on glycerol whereas the others (*a*S_{175}D, *a*S_{175}K, *a*P_{12}S, *a*I_{239}F, and *a*I_{171}N) resulted in a slow respiratory growth phenotype, at all temperatures tested (20°C, 28°C, 36°C) (shown for 28°C in Fig. 2A,B)). All the revertants had a much better genetic stability than the *a*S_{175}N mutant as evidenced by a reduced accumulation of ρ^-/ρ^o cells in cultures (10% or less vs 35%) (Table 3).

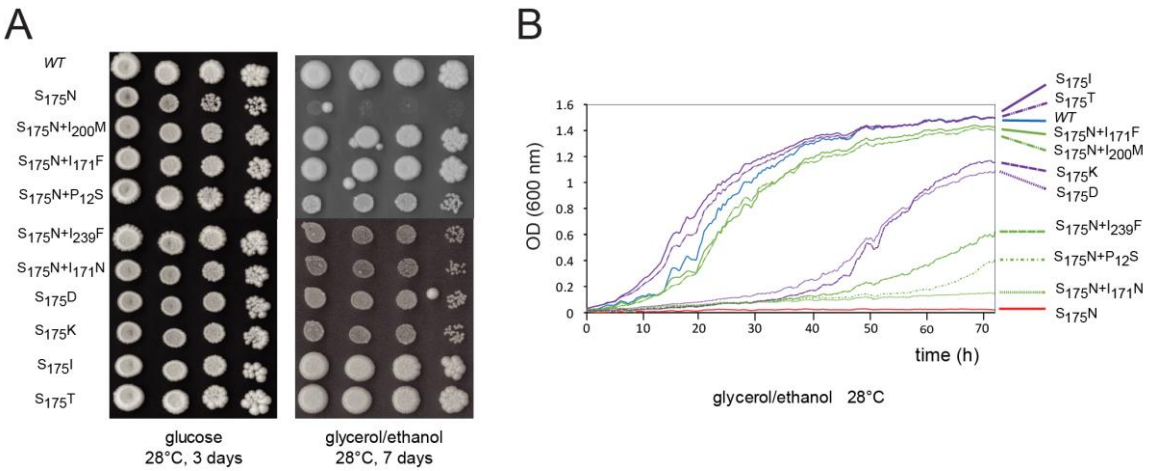

Figure 2. Growth of mutant strains. (A) Fresh liquid glucose cultures of wild type yeast, mutant *a*S_{175}N and its revertants were serially diluted and spotted on rich glucose and rich glycerol/ethanol plates. The glucose and glycerol plates were photographed after 3 and 7 days of incubation at 28°C, respectively. (B) Growth curves in liquid rich glycerol/ethanol at 28°C.

3.2.2. Respiration and ATP synthesis

Improvement of ATP synthase function by the suppressors was evaluated first by measuring oxygen consumption and ATP synthesis rates in isolated mitochondria. As shown previously, yeast *atp6* mutations including *a*S_{175}N that compromise ATP synthase activity usually result in a diminished respiration rate mainly because of a lower content in complex IV ([15, 29, 33, 45] Table 3). Thus, decreased ATP synthesis rate in *atp6* mutants is not primarily due to a reduced rate of electron transfer to oxygen but to some defect in the ATP synthase that secondarily impacts respiration. Oxygen consumption was assessed with NADH as an electron donor, alone (basal, state 4 respiration), after further addition (75 μM) of ADP (state 3, phosphorylating conditions) or in the presence of the membrane proton ionophore CCCP (carbonyl cyanide *m*-chlorophenylhydrazone) (uncoupled respiration). Under state 4, respiration is controlled by the passive permeability to protons of the inner membrane. Under state 3, most of the protons return to the matrix through the ATP synthase so that the contribution to respiration of passive proton leaks becomes very small. In the presence of CCCP, the maintenance of an electrical potential (ΔΨ) across the inner membrane is impossible and respiration becomes maximal. We also measured complex IV activity using ascorbate/TMPD (N,N,N′,N′-tetramethyl-phenylenediamine) in the presence of CCCP. Mitochondrial ATP synthesis rate was measured using NADH as a respiratory substrate in the presence of a large excess (750 μM) of external ADP, conditions under which ATP is synthesized exclusively by ATP synthase using the proton-motive force generated by complexes III and IV (there is no complex I in *S. cerevisiae*).

Consistent with their good growth on glycerol, mitochondria from strains *a*S_{175}I, *a*S_{175}T, *a*S_{175}N+*a*I_{171}F and *a*S_{175}N+*a*I_{200}M efficiently respired and produced ATP almost like those from wild type yeast (Table 3). Accordingly, in all the slowly growing revertants ATP synthesis rate was diminished by 80-90% compared to the *WT*. ATP synthase assembled and accumulated quite efficiently in all the revertants (Fig. 3). Regarding the Westerns with Atp6 antibodies, it apparently seems that there is much less ATP synthase in the *a*P_{12}S revertant whereas the Atp1 antibodies did not reveal a lack of this enzyme in this strain. The most likely explanation is that the *a*P_{12}S mutation is within the sequence of subunit *a* (a.a. 11-23) that we used to raise the Atp6 antibodies, and that because of this these antibodies reacted less efficiently with the *a*P_{12}S subunit.

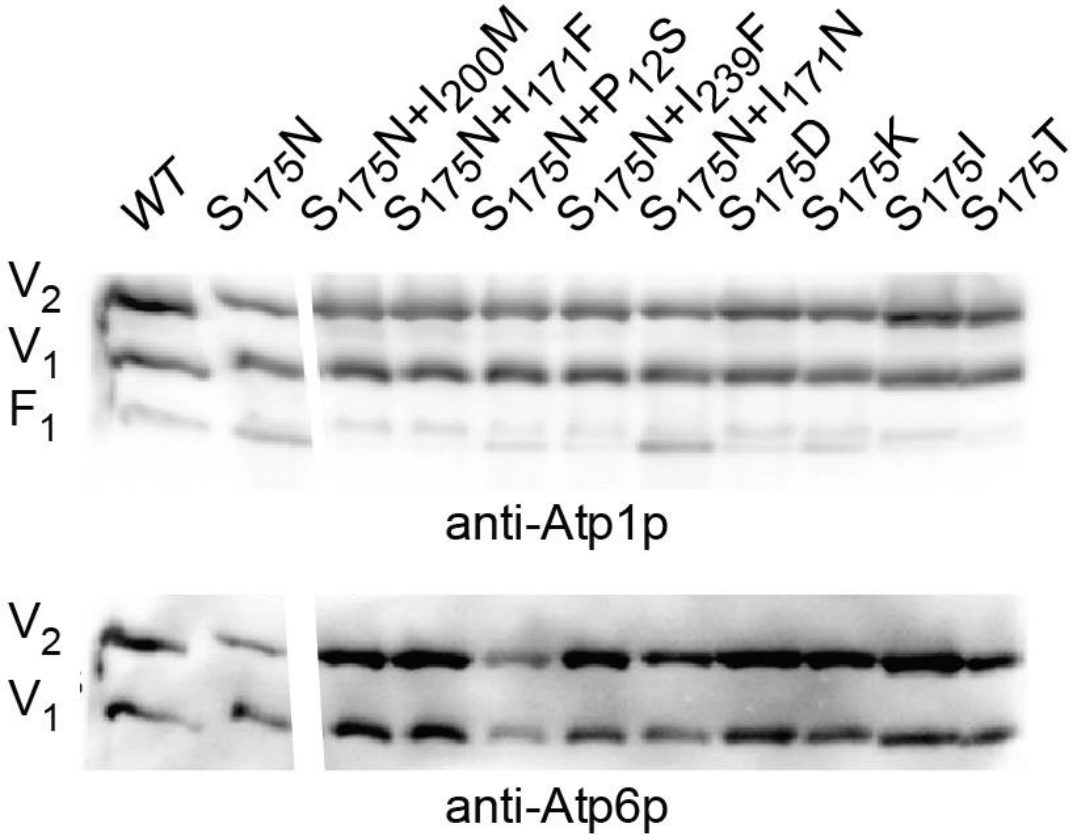

Figure 3. Levels of ATP synthase in the revertants. Proteins were extracted from the mitochondrial samples used in the bioenergetics experiments described in Table 3 with 1.5 gr digitonin per gr of proteins and separated by BN-PAGE (200 µg per lane). The proteins were transferred onto PVDF membrane and probed with antibodies against subunit *a* (Atp6) or F1-subunit Atp1 of ATP synthase, revealing dimeric (V_2) and monomeric (V_1) F_1F_O complexes. The shown Westerns are representative of three independent experiments.

3.2.3. Membrane potential

The influence of the suppressor mutations was investigated further using Rhodamine 123, a fluorescent cationic dye that can be used to monitor changes in mitochondrial membrane potential (ΔΨ) [37]. Increasing ΔΨ is followed by the uptake of the dye inside the matrix and concomitant fluorescence quenching. In a first set of experiments (Fig. 4A), we tested the capacity of externally added ADP to induce ΔΨ consumption. To this end, mitochondria were first fed with electrons from ethanol. Due to their strongly reduced capacity to respire, those from the mutant *a*S_{175}N were poorly energized in comparison to *WT* mitochondria whereas ethanol induced a much larger ΔΨ variation in all the revertants. Normally, further adding a small amount of ADP induces a transient fluorescence increase due to ΔΨ consumption by the ATP synthase during phosphorylation of the added ADP. This was indeed observed in mitochondria from the *WT* and the revertants, whereas those from the *a*S_{175}N mutant were virtually insensitive to ADP consistent with their very poor capacity to produce ATP (Table 3). However, in those revertants growing slowly on glycerol (*a*S_{175}D, *a*S_{175}K, *a*S_{175}N+*a*P_{12}S, *a*S_{175}N+*a*I_{239}F, and *a*S_{175}N+*a*I_{171}N) a much longer time was needed to recover the ethanol-induced ΔΨ compared to the *WT* and the revertants

with a good growth on glycerol ($aS_{175}I$, $aS_{175}T$, $aS_{175}N+aI_{171}F$, and $aS_{175}N+aI_{200}M$), reflecting the large differences in ATP synthesis rate between these strains. KCN was then added to inhibit complex IV, which, in mitochondria from the *WT* and the revertants resulted in a partial ΔΨ collapse. The remaining potential was due to F_O-mediated proton pumping coupled to hydrolysis of the ATP that accumulated in the mitochondrial matrix during phosphorylation of the added ADP, as evidenced by the loss of this potential by inhibiting ATP synthase with oligomycin. By contrast, no oligomycin-sensitive ΔΨ was observed in the $aS_{175}N$ mitochondria owing to their incapacity to produce ATP.

In a second set of experiments (Fig. 4B), we directly tested the proton-pumping activity of ATP synthase using externally added ATP independently of the respiratory chain. To this end, mitochondria were first energized with ethanol to remove the natural inhibitory peptide (IF1) of F_1-ATPase. ΔΨ was then collapsed with KCN, and less than one minute later, thus well before IF1 rebinding [46], ATP was added. External ATP is counter-exchanged against ADP present in the matrix by the ADP/ATP translocase, which does not require any ΔΨ, and the ATP can then be hydrolyzed by F_1 coupled to F_O-mediated proton transport. Adding ATP promoted in mitochondria from the *WT* and the revertants a large and stable fluorescence quenching of the dye that was reversed upon inhibition with oligomycin, whereas $aS_{175}N$ mitochondria were mostly insensitive to ATP due to their inability to move protons through the F_O.

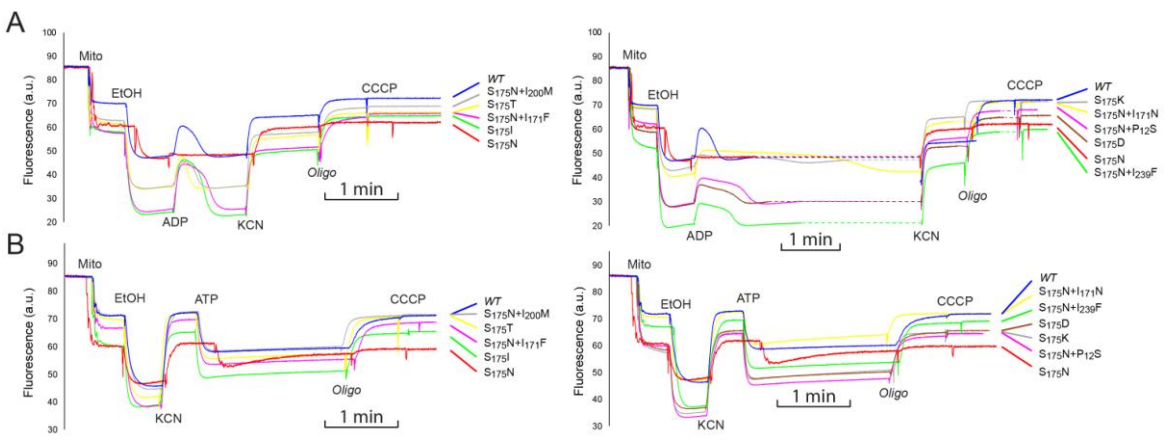

Figure 4. Mitochondrial membrane potential. Variations in mitochondrial ΔΨ were monitored by fluorescence quenching of Rhodamine 123 in the mitochondria used for the bioenergetics experiments described in Table 3. The tracings in panel A show how the mitochondria respond to the addition of ADP, those in panel B reflect the proton-pumping activity of ATP synthase. The additions were 75 µM ADP, 0.5 µg/ml Rhodamine 123, 75 µg/mL mitochondrial proteins (Mito), 10 µL ethanol (EtOH), 2 mM potassium cyanide (KCN), 4 µg/mL oligomycin (oligo), and 4 µM carbonyl cyanide-m-chlorophenyl hydrazone (CCCP). The shown tracings are representative of three experiments.

3.3. Topological location of the mutations

The locations in the recently published atomic structure of yeast F_O [5] of the mutations here described (*a*S_{175}N, *a*S_{175}D, *a*S_{175}K, *a*S_{175}I, *a*S_{175}N, *a*P_{12}S, *a*I_{171}F, *a*I_{171}N, *a*I_{239}F, and *a*I_{200}M) are shown in Fig. 5. The amino acid alignments in Fig. 1 establish the correspondences with human subunit *a* residues. The six membrane-associated helices of subunit *a* and the two transmembrane helices of subunit *c* are referred to as *a*H1-6 and *c*TM1-2 respectively (Fig. 5A). At the interface between the *a*-subunit and the *c*-ring, near the middle of the membrane, are two electrically charged residues (*a*R_{186} and *c*E_{59}) directly involved in proton translocation. Being kinked, *a*H5 (residues 162-209) can follow the curvature of the *c*-ring and seal the two hydrophilic pockets that connect the *a*/c-ring interface to the intermembrane and matrix spaces. The N-term part of *a*H5 (residues 162-180, 31 Å long) is shorter than its C-term part (residues 184-209, 43 Å long), and *a*H6 (residues 219-257, 55 Å) is shorter and more straight than *a*H5, which creates a funnel-shaped cleft between subunit *a* and the *c*-ring accessible from the matrix (Fig. 5B). The mouth of this cleft

is surrounded by a short helix *a*Hβ (residues 137-147) that connects *a*H4 and *a*H5, the C-terminal extremity of subunit *a*, and a five amino acid long loop (residues 85-89) between *a*H2 and *a*H3. The cleft, into which points the essential aR_{186} residue, is 15 Å long (from aR_{186} to aD_{254} or E_{172}), 8 Å wide (from aD_{254} to aE_{172}) and 16 Å deep (from aS_{175} to the C-terminus of the protein). It is bordered by polar or electrically charged residues on *a*H5 (aS_{250}, $aY_{25}1$, aK_{253}, aD_{254}, aH_{259}) and *a*H6 (aE_{172}, aS_{175}, aR_{179}, aS_{182}), two of which, aE_{172} and aD_{254}, would be essential for moving protons out of the cleft [5, 34] (Fig. 5B,D). Since the others, as well as those surrounding cE_{59} (cF_{48}, cP_{49}, cI_{52}, cL_{53}, cF_{55}, cA_{56}, cL_{57}), cannot engage in hydrogen bonding, it is possible that water molecules inside the cleft help proton conduction towards the matrix.

Although aS_{175} is highly conserved (Fig. 1), has a hydroxyl group that can exchange protons and is located in the *n*-side cleft, this residue is clearly not required for F_O-mediated proton translocation. Indeed, as shown in this study, ATP synthase function was fully preserved with the presence at position 175 of an aliphatic side chain residue (*a*I175). These findings are in line with a previous study showing that replacing the equivalent serine in subunit *a* of *E. coli* by alanine had no detrimental consequences [47]. aI_{175} can orient towards the *c*-ring without any steric hindrance on E_{172} and preserve with aL_{164}, aL_{167} and aI_{171} a non-polar environment around the *c*-ring (Fig. 5D). The absence of major functional defects with a threonine residue at position 175 (aT_{175}) further supports a non-essential role for aS_{175}.

Disruption of F_O-mediated proton transport induced by aN_{175} possibly results from the establishment of two hydrogen bonds between aN_{175} amide and aE_{172} carboxylate groups that are distant by 3.1 and 3.3 Å (Fig. 5B,C). As a result the glutamate would become unable to conduct protons out of the *n*-side cleft.

Alternatively, *a*N_{175} can orient towards the *c*-ring without making a direct hydrogen bond with the catalytic *c*E_{59} residue (because of a too long distance, 4 Å) (Fig. 5D). However, it will then impair rotation of the *c*-ring by clashing *c*A_{56} and *c*L_{57}. Like *a*N_{175}, *a*D_{175} can adopt the same two orientations towards either *a*E_{172} or the *c*-ring. However the electrostatic repulsion between *a*D_{175} and *a*E_{172} most likely favors the second one, which may explain the recovery of ATP synthase function when *a*N_{175} is replaced by aspartate. The poor suppressor activity of *a*D_{175} is possibly due to clashes with the *c*-ring and/or unproductive proton transfers. The suppressor activity of *a*K_{175} probably also result from the recovery of *a*E_{172} to conduct protons. Owing to its flexibility and hydrophobic alkyl moiety, the lysine side chain may easily adopt a conformation that preserves *c*-ring rotation. However due to its positive charge, a reduced strength of attraction for protons towards the matrix may be responsible for the slow and inefficient functioning of ATP synthase with *a*K_{175}.

The five-second site suppressors that make the *a*S_{175}N mutation no longer or less detrimental all localize close to the *a*/*c* interface (Fig. 5E,F). Two are in proximity to the original mutation, at position 171 (*a*I_{171}F and *a*I_{171}N). ATP synthase function was fully restored with *a*F_{171}. Replacement of *a*I_{171} by a rigid and bulkier phenylalanine group may structurally shift the position of *a*N_{175} towards the *c*-ring so as it can no longer interact with *a*E_{172} without affecting the sealing of the two hydrophilic pockets by *a*H5. Furthermore, as a highly hydrophobic residue, phenylalanine preserves the non-polar surface that *a*H5 (*a*L_{164}, *a*L_{167}, *a*L_{168}, *a*I_{171}, *a*L_{174}, *a*A_{178}, *a*A_{193}, *a*L_{197}, *a*I_{200}, *a*L_{201}, and *a*L_{204}) and *a*H6 (*a*M_{225}, *a*I_{229}, *a*L_{232}, *a*I_{236}, *a*I_{239}) provide in front of the *c*-ring so as to ease its rotation. The suppressor activity of *a*N_{171} is much less efficient compared to *a*F_{171}, indicating that *a*N_{175} remains mostly

bound to *a*E_{172} and that the proton exchanging capacity of *a*N_{171} helps somehow the protons to quit the *c*-ring.

The three other second-site suppressors are remotely located from the original *a*S_{175}N mutation, by 35 Å (*a*P_{12}S, *a*I_{200}M) or 23 Å (*a*I_{239}F) on the *p*-side of the membrane (Fig. 5E). They are quite close to conserved residues presumably involved in the transport of protons from the intermembrane space (*a*E_{233} (H in *E. coli*), *a*N_{190}, *a*Q_{240} and *a*H_{195} (E in *E. coli*)) to *a*R_{186}. Interestingly, the *a*P_{12}S suppressor belongs to a region of subunit *a* that does not exist in bovine and humans (Fig. 1). That it can upon mutation compensate for the *a*S_{175}N change indicates that this region has an important function in yeast ATP synthase. Consistently, this region shows a rather good amino acid sequence conservation in those mitochondria where it is present. While it is difficult to provide a mechanistic explanation for these long-distance interactions that improve F_O-mediated proton transfer in the *a*S_{175}N mutant this is, as discussed below, an interesting observation.

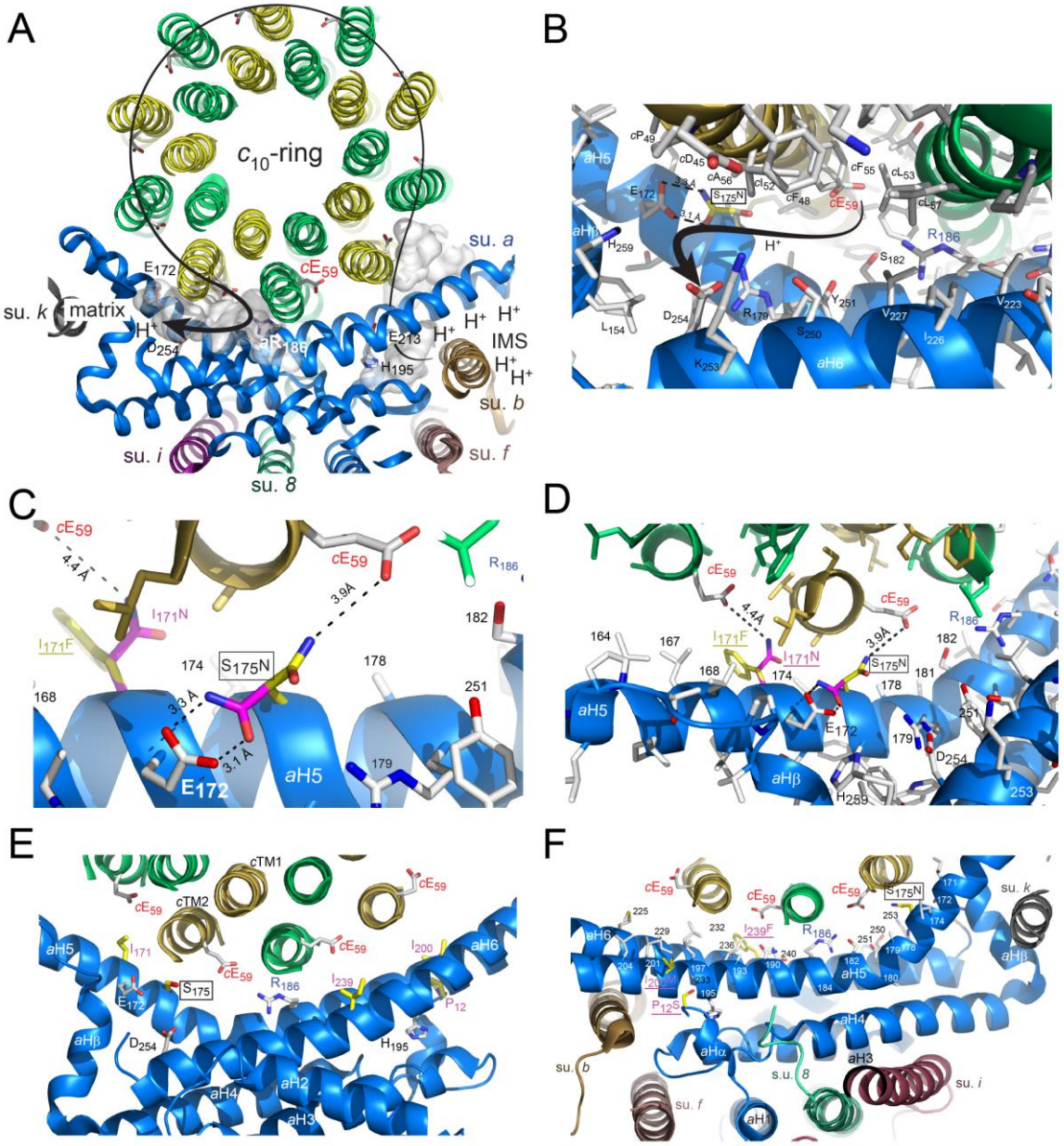

443

444 **Figure 5**. **Topological locations of the mutations.** (A) View of the entire *c*-ring and
445 subunit *a* from the matrix and of the pathway along which protons are transported
446 from the intermembrane space to the mitochondrial matrix. The side chains of the two
447 residues essential to this transfer (aR_{186} and cE_{59}) are drawn as stick with their
448 carbon atoms in white. The *p*-side and *n*-side clefts are shown as grey surface. (B)
449 The original $aS_{175}N$ mutation prevents by hydrogen bonding the nearby glutamate
450 aE_{172} to move protons out the *n*-side cleft. (C) Zoom on the hydrogen bonds that

aN$_{175}$ can potentially form with aE$_{172}$ (D) View from the matrix showing the two possible orientations of aN$_{175}$ towards either the *c*-ring (yellow) or aE$_{172}$ (magenta). aF$_{171}$ (yellow) is supposed to orient aN$_{175}$ towards the *c*-ring, thus restoring the proton conducting activity of aE$_{172}$, whereas aN$_{175}$ remains oriented towards aE$_{172}$ with aN$_{171}$ (magenta). (E) Enlargement of the region showing the five mutated residues (aS$_{175}$, aP$_{12}$, aI$_{171}$, aI$_{200}$, and aI$_{239}$); their side chains are drawn as stick with their carbon atoms in yellow. Residues presumed to be important for proton transfer (aE$_{172}$, aD$_{234}$, aH$_{195}$ and aD$_{254}$) are represented as stick with their carbon atoms in white color. (F) Enlargement around the aP$_{12}$S, aI$_{200}$M and aI$_{239}$F second-site suppressors.

4. Conclusion

With the recently described cryo-EM structures of F_1F_O ATP synthase from various mitochondrial origins it has become feasible to map at a molecular level discrete structural changes of this enzyme found to be responsible for human diseases. Although this is a major step towards a better comprehension of these diseases, it is generally difficult to understand how loss-of-function mutations act. The suppressor genetics approach used in this study help to understand how a pathogenic mutation in subunit *a* (aS$_{148}$N in humans, aS$_{175}$N in yeast) disrupts F_O-mediated proton conduction. Our results reveal that despite its very strong evolutionary conservation and its capacity to exchange protons thanks to the presence of a hydroxyl group on its side chain, the mutated serine is by itself not directly involved in this activity. Indeed, consistent with a previous study in *E. coli* [47], ATP synthase function was fully regained by replacing the mutant asparagine with aliphatic residues that do not have the capacity to conduct protons. Thus, losing the serine is by itself not problematic, it is its replacement by asparagine that leads to the loss of F_O function.

476 The most likely explanation that emerges from our suppressor genetic analysis and
477 the atomic structure of yeast F_O, is that the mutant asparagine neutralizes by
478 hydrogen bonding the nearby glutamate (aE$_{172}$) presumed to be critical for the exit of
479 protons from the *n*-side hydrophilic cleft.

480 Very interestingly also, we show that the serine-to-asparagine change can be
481 somewhat efficiently suppressed by mutations in other positions of subunit *a*
482 (second-site suppressors). Thus, while being still present, the mutant asparagine
483 ceases to be or is much less detrimental. Surprisingly, some of the second-site
484 suppressors are within the *p*-side cleft that provides a pathway for protons from the
485 intermembrane space. These suppressors must thus be responsible for long (20-30
486 Å)-range effects that somehow disrupt the detrimental hydrogen bound between
487 aE$_{172}$ and aN$_{175}$ or help the protons to find another route to reach the mitochondrial
488 matrix. It is not unreasonable to imagine that drugs could as well undo an
489 undesirable hydrogen bond by hitting the regions of subunit *a* modified by the
490 suppressors. The approach used in this study is not only helpful to better understand
491 how mutations of ATP synthase induce diseases, but may also open the door to
492 drug-design therapeutic developments.
493
494

Acknowledgements

This work was supported by grants from National Science Center of Poland (2016/23/B/NZ3/02098) to R.K, AFM (Association Française contre les Myopathies) to J.-P.dR, Agence Nationale de la Recherche to M.-F.G. (ANR-12-BSV8-024), National Natural Science Foundation (NSF) Grant (81370788 & 8151101098) to H.C. N.S. and K.B. were supported by the Polonium grant 35301WC, Ministère Français de l'Enseignement Supérieur et de la Recherche, and Ministry of Science and Higher Education of Poland.

Author Contributions

N.S., K.B., F.G., M.B., S.X., J.-P.L., D.T.-T., and H.C. isolated the revertants and analyzed their properties; A.D. performed the structural modeling analyses with a financial support provided by M.-F. G.; J.-P.dR. and R.K. designed the research; A.D., R.K. and J.-P.dR wrote the paper.

References

[1] P.D. Boyer, The ATP synthase--a splendid molecular machine, Annu. Rev. Biochem., 66 (1997) 717-749.

[2] A. Hahn, K. Parey, M. Bublitz, D.J. Mills, V. Zickermann, J. Vonck, W. Kuhlbrandt, T. Meier, Structure of a Complete ATP Synthase Dimer Reveals the Molecular Basis of Inner Mitochondrial Membrane Morphology, Mol. Cell., 63 (2016) 445-456.

[3] E. Morales-Rios, I.N. Watt, Q. Zhang, S. Ding, I.M. Fearnley, M.G. Montgomery, M.J. Wakelam, J.E. Walker, Purification, characterization and crystallization of the F-ATPase from Paracoccus denitrificans, Open Biol., 5 (2015) 150119.

[4] A. Zhou, A. Rohou, D.G. Schep, J.V. Bason, M.G. Montgomery, J.E. Walker, N. Grigorieff, J.L. Rubinstein, Structure and conformational states of the bovine mitochondrial ATP synthase by cryo-EM, eLife, 4 (2015).

[5] H. Guo, S.A. Bueler, J.L. Rubinstein, Atomic model for the dimeric FO region of mitochondrial ATP synthase, Science, 358 (2017) 936-940.

[6] M. Allegretti, N. Klusch, D.J. Mills, J. Vonck, W. Kuhlbrandt, K.M. Davies, Horizontal membrane-intrinsic alpha-helices in the stator a-subunit of an F-type ATP synthase, Nature, 521 (2015) 237-240.

[7] M. Strauss, G. Hofhaus, R.R. Schroder, W. Kuhlbrandt, Dimer ribbons of ATP synthase shape the inner mitochondrial membrane, EMBO j., 27 (2008) 1154-1160.

[8] K.M. Davies, M. Strauss, B. Daum, J.H. Kief, H.D. Osiewacz, A. Rycovska, V. Zickermann, W. Kuhlbrandt, Macromolecular organization of ATP synthase and complex I in whole mitochondria, Proc. Natl. Acad. Sci. U.S.A., 108 (2011) 14121-14126.

[9] S.B. Vik, B.J. Antonio, A mechanism of proton translocation by F1F0 ATP synthases suggested by double mutants of the a subunit, J. Biol. Chem., 269 (1994) 30364-30369.
[10] W. Junge, H. Lill, S. Engelbrecht, ATP synthase: an electrochemical transducer with rotatory mechanics, Trends Biochem. Sci., 22 (1997) 420-423.
[11] N. Mitome, S. Ono, H. Sato, T. Suzuki, N. Sone, M. Yoshida, Essential arginine residue of the F(o)-a subunit in F(o)F(1)-ATP synthase has a role to prevent the proton shortcut without c-ring rotation in the F(o) proton channel, Biochem. J., 430 (2010) 171-177.
[12] D. Pogoryelov, A. Krah, J.D. Langer, O. Yildiz, J.D. Faraldo-Gomez, T. Meier, Microscopic rotary mechanism of ion translocation in the F(o) complex of ATP synthases, Nature Chem. Biol., 6 (2010) 891-899.
[13] E. Morales-Rios, M.G. Montgomery, A.G. Leslie, J.E. Walker, Structure of ATP synthase from Paracoccus denitrificans determined by X-ray crystallography at 4.0 A resolution, Proc. Natl. Acad. Sci. U.S.A., 112 (2015) 13231-13236.
[14] J.P. Abrahams, A.G. Leslie, R. Lutter, J.E. Walker, Structure at 2.8 A resolution of F1-ATPase from bovine heart mitochondria, Nature, 370 (1994) 621-628.
[15] R. Kucharczyk, M. Zick, M. Bietenhader, M. Rak, E. Couplan, M. Blondel, S.D. Caubet, J.P. di Rago, Mitochondrial ATP synthase disorders: molecular mechanisms and the quest for curative therapeutic approaches, Biochim. Biophys. Acta., 1793 (2009) 186-199.
[16] F.J. Miller, F.L. Rosenfeldt, C. Zhang, A.W. Linnane, P. Nagley, Precise determination of mitochondrial DNA copy number in human skeletal and cardiac muscle by a PCR-based assay: lack of change of copy number with age, Nuc. Acids Res., 31 (2003) e61.
[17] L.M. Steinmetz, C. Scharfe, A.M. Deutschbauer, D. Mokranjac, Z.S. Herman, T. Jones, A.M. Chu, G. Giaever, H. Prokisch, P.J. Oefner, R.W. Davis, Systematic screen for human disease genes in yeast, Nat. Genet., 31 (2002) 400-404.
[18] J. Reinders, R.P. Zahedi, N. Pfanner, C. Meisinger, A. Sickmann, Toward the complete yeast mitochondrial proteome: multidimensional separation techniques for mitochondrial proteomics, J Proteome Res., 5 (2006) 1543-1554.
[19] H. Prokisch, C. Scharfe, D.G. Camp, 2nd, W. Xiao, L. David, C. Andreoli, M.E. Monroe, R.J. Moore, M.A. Gritsenko, C. Kozany, K.K. Hixson, H.M. Mottaz, H. Zischka, M. Ueffing, Z.S. Herman, R.W. Davis, T. Meitinger, P.J. Oefner, R.D. Smith, L.M. Steinmetz, Integrative analysis of the mitochondrial proteome in yeast, PLoS Biol., 2 (2004) e160.
[20] D.J. Pagliarini, S.E. Calvo, B. Chang, S.A. Sheth, S.B. Vafai, S.E. Ong, G.A. Walford, C. Sugiana, A. Boneh, W.K. Chen, D.E. Hill, M. Vidal, J.G. Evans, D.R. Thorburn, S.A. Carr, V.K. Mootha, A mitochondrial protein compendium elucidates complex I disease biology, Cell, 134 (2008) 112-123.
[21] H.W. Rhee, P. Zou, N.D. Udeshi, J.D. Martell, V.K. Mootha, S.A. Carr, A.Y. Ting, Proteomic mapping of mitochondria in living cells via spatially restricted enzymatic tagging, Science, 339 (2013) 1328-1331.
[22] N. Bonnefoy, T.D. Fox, Genetic transformation of Saccharomyces cerevisiae mitochondria, Meth. Cell Biol., 65 (2001) 381-396.
[23] K. Okamoto, P.S. Perlman, R.A. Butow, The sorting of mitochondrial DNA and mitochondrial proteins in zygotes: preferential transmission of mitochondrial DNA to the medial bud, J. Cell Biol., 142 (1998) 613-623.
[24] M.G. Baile, S.M. Claypool, The power of yeast to model diseases of the powerhouse of the cell, Front. Biosci. (Landmark Ed), 18 (2013) 241-278.
[25] J.P. Lasserre, A. Dautant, R.S. Aiyar, R. Kucharczyk, A. Glatigny, D. Tribouillard-Tanvier, J. Rytka, M. Blondel, N. Skoczen, P. Reynier, L. Pitayu, A. Rotig, A. Delahodde, L.M. Steinmetz, G. Dujardin, V. Procaccio, J.P. di Rago, Yeast as a system for modeling mitochondrial disease mechanisms and discovering therapies, D.M.M., 8 (2015) 509-526.
[26] A.M. Kabala, J.P. Lasserre, S.H. Ackerman, J.P. di Rago, R. Kucharczyk, Defining the impact on yeast ATP synthase of two pathogenic human mitochondrial DNA mutations, T9185C and T9191C, Biochimie, 100 (2014) 200-206.

[27] R. Kucharczyk, N. Ezkurdia, E. Couplan, V. Procaccio, S.H. Ackerman, M. Blondel, J.P. di Rago, Consequences of the pathogenic T9176C mutation of human mitochondrial DNA on yeast mitochondrial ATP synthase, Biochim. Bioph. Acta, 1797 (2010) 1105-1112.

[28] R. Kucharczyk, M.F. Giraud, D. Brethes, M. Wysocka-Kapcinska, N. Ezkurdia, B. Salin, J. Velours, N. Camougrand, F. Haraux, J.P. di Rago, Defining the pathogenesis of human mtDNA mutations using a yeast model: the case of T8851C, Int. J. Biochem. Cell Biol., 45 (2013) 130-140.

[29] R. Kucharczyk, M. Rak, J.P. di Rago, Biochemical consequences in yeast of the human mitochondrial DNA 8993T>C mutation in the ATPase6 gene found in NARP/MILS patients, Biochim. Biophys. Acta, 1793 (2009) 817-824.

[30] R. Kucharczyk, B. Salin, J.P. di Rago, Introducing the human Leigh syndrome mutation T9176G into Saccharomyces cerevisiae mitochondrial DNA leads to severe defects in the incorporation of Atp6p into the ATP synthase and in the mitochondrial morphology, Hum. Mol. Genet., 18 (2009) 2889-2898.

[31] K. Niedzwiecka, A.M. Kabala, J.P. Lasserre, D. Tribouillard-Tanvier, P. Golik, A. Dautant, J.P. di Rago, R. Kucharczyk, Yeast models of mutations in the mitochondrial ATP6 gene found in human cancer cells, Mitochondrion, 29 (2016) 7-17.

[32] M. Rak, E. Tetaud, S. Duvezin-Caubet, N. Ezkurdia, M. Bietenhader, J. Rytka, J.P. di Rago, A yeast model of the neurogenic ataxia retinitis pigmentosa (NARP) T8993G mutation in the mitochondrial ATP synthase-6 gene, J. Biol. Chem., 282 (2007) 34039-34047.

[33] S. Wen, K. Niedzwiecka, W. Zhao, S. Xu, S. Liang, X. Zhu, H. Xie, D. Tribouillard-Tanvier, M.F. Giraud, C. Zeng, A. Dautant, R. Kucharczyk, Z. Liu, J.P. di Rago, H. Chen, Identification of G8969>A in mitochondrial ATP6 gene that severely compromises ATP synthase function in a patient with IgA nephropathy, Sci. Rep., 6 (2016) 36313.

[34] A.P. Srivastava, M. Luo, W. Zhou, J. Symersky, D. Bai, M.G. Chambers, J.D. Faraldo-Gomez, M. Liao, D.M. Mueller, High-resolution cryo-EM analysis of the yeast ATP synthase in a lipid membrane, Science, (2018)

[35] B. Guerin, P. Labbe, M. Somlo, Preparation of yeast mitochondria (Saccharomyces cerevisiae) with good P/O and respiratory control ratios, Meth. Enzym., 55 (1979) 149-159.

[36] M. Rigoulet, B. Guerin, Phosphate transport and ATP synthesis in yeast mitochondria: effect of a new inhibitor: the tribenzylphosphate, FEBS Letters, 102 (1979) 18-22.

[37] R.K. Emaus, R. Grunwald, J.J. Lemasters, Rhodamine 123 as a probe of transmembrane potential in isolated rat-liver mitochondria: spectral and metabolic properties, Biochim. Biophys. Acta, 850 (1986) 436-448.

[38] H. Schagger, G. von Jagow, Blue native electrophoresis for isolation of membrane protein complexes in enzymatically active form, Anal. Biochem., 199 (1991) 223-231.

[39] I. Bohovych, O. Khalimonchuk, Sending Out an SOS: Mitochondria as a Signaling Hub, Front. Cell Dev. Biol., 4 (2016) 109.

[40] V. Contamine, M. Picard, Maintenance and integrity of the mitochondrial genome: a plethora of nuclear genes in the budding yeast, M.M.B.R., 64 (2000) 281-315.

[41] J.P. di Rago, P. Netter, P.P. Slonimski, Pseudo-wild type revertants from inactive apocytochrome b mutants as a tool for the analysis of the structure/function relationships of the mitochondrial ubiquinol-cytochrome c reductase of Saccharomyces cerevisiae, J. Biol. Chem., 265 (1990) 3332-3339.

[42] T. Michon, M. Galante, J. Velours, NH2-terminal sequence of the isolated yeast ATP synthase subunit 6 reveals post-translational cleavage, Eur. J. Biochem. / FEBS, 172 (1988) 621-625.

[43] S. Liu, T.J. Charlesworth, J.V. Bason, M.G. Montgomery, M.E. Harbour, I.M. Fearnley, J.E. Walker, The purification and characterization of ATP synthase complexes from the mitochondria of four fungal species, Biochem. J., 468 (2015) 167-175.

[44] M. Sobti, C. Smits, A.S. Wong, R. Ishmukhametov, D. Stock, S. Sandin, A.G. Stewart, Cryo-EM structures of the autoinhibited E. coli ATP synthase in three rotational states, eLife, 5 (2016).

[45] M. Bietenhader, A. Martos, E. Tetaud, R.S. Aiyar, C.H. Sellem, R. Kucharczyk, S. Clauder-Munster, M.F. Giraud, F. Godard, B. Salin, I. Sagot, J. Gagneur, M. Dequard-Chablat, V. Contamine, S. Hermann-Le Denmat, A. Sainsard-Chanet, L.M. Steinmetz, J.P. di Rago, Experimental relocation of the mitochondrial ATP9 gene to the nucleus reveals forces underlying mitochondrial genome evolution, PLoS Genet., 8 (2012) e1002876.

[46] R. Venard, D. Brethes, M.F. Giraud, J. Vaillier, J. Velours, F. Haraux, Investigation of the role and mechanism of IF1 and STF1 proteins, twin inhibitory peptides which interact with the yeast mitochondrial ATP synthase, Biochemistry, 42 (2003) 7626-7636.

[47] S.B. Vik, B.D. Cain, K.T. Chun, R.D. Simoni, Mutagenesis of the alpha subunit of the F1Fo-ATPase from Escherichia coli. Mutations at Glu-196, Pro-190, and Ser-199, J. Biol. Chem., 263 (1988) 6599-6605.

[48] M. Rak, E. Tetaud, F. Godard, I. Sagot, B. Salin, S. Duvezin-Caubet, P.P. Slonimski, J. Rytka, J.P. di Rago, Yeast cells lacking the mitochondrial gene encoding the ATP synthase subunit 6 exhibit a selective loss of complex IV and unusual mitochondrial morphology, J. Biol. Chem., 282 (2007) 10853-10864.

[49] J.P. van Dijken, J. Bauer, L. Brambilla, P. Duboc, J.M. Francois, C. Gancedo, M.L. Giuseppin, J.J. Heijnen, M. Hoare, H.C. Lange, E.A. Madden, P. Niederberger, J. Nielsen, J.L. Parrou, T. Petit, D. Porro, M. Reuss, N. van Riel, M. Rizzi, H.Y. Steensma, C.T. Verrips, J. Vindelov, J.T. Pronk, An interlaboratory comparison of physiological and genetic properties of four Saccharomyces cerevisiae strains, Enz. Microb. Technn., 26 (2000) 706-714.

[50] D.F. Steele, C.A. Butler, T.D. Fox, Expression of a recoded nuclear gene inserted into yeast mitochondrial DNA is limited by mRNA-specific translational activation, Proc. Natl. Acad. Sci. U.S.A., 93 (1996) 5253-5257.

Table 1. Genotypes and origins of yeast strains.

Strain	Nuclear genotype	mtDNA	Source
MR6	*MATa ade2-1 his3-11,15 trp1-1 leu2-3,112 ura3-1 CAN1 arg8::HIS3*	ρ^+	[48]
D273-10B/60	*Matα met6*	ρ^o	[49]
DFS160	*MATα leu2Δ ura3-52 ade2-101 arg8::URA3 kar1-1*	ρ^o	[50]
NB40-3C	*MATa lys2 leu2-3,112 ura3-52 his3ΔHindIII arg8::hisG*	ρ^+ *cox2-62*	[49]
MR10	*MATa ade2-1 his3-11,15 trp1-1 leu2-3,112 ura3-1 CAN1 arg8::hisG*	ρ^+ *atp6::ARG8*^{m}	[48]
RKY105	*MATa ade2-1 his3-11,15 trp1-1 leu2-3,112 ura3-1 CAN1 arg8::HIS3*	ρ^+ *atp6*-$S_{175}N$	This study
RKY105-R1/3	*MATa ade2-1 his3-11,15 trp1-1 leu2-3,112 ura3-1 CAN1 arg8::HIS3*	ρ^+*atp6*-$I_{171}F$+$S_{175}N$	This study
RKY105-R1/4	*MATa ade2-1 his3-11,15 trp1-1 leu2-3,112 ura3-1 CAN1 arg8::HIS3*	ρ^+*atp6*-$I_{239}F$+$S_{175}N$	This study
RKY105-R2/3	*MATa ade2-1 his3-11,15 trp1-1 leu2-3,112 ura3-1 CAN1 arg8::HIS3*	ρ^+*atp6*-$I_{200}M$+$S_{175}N$	This study
RKY105-R2/5	*MATa ade2-1 his3-11,15 trp1-1 leu2-3,112 ura3-1 CAN1 arg8::HIS3*	ρ^+*atp6*-$P_{12}S$+$S_{175}N$	This study
RKY105-R6/5	*MATa ade2-1 his3-11,15 trp1-1 leu2-3,112 ura3-1 CAN1 arg8::HIS3*	ρ^+*atp6*-$S_{175}K$	This study
RKY105-R9/2	*MATa ade2-1 his3-11,15 trp1-1 leu2-3,112 ura3-1 CAN1 arg8::HIS3*	ρ^+*atp6*-$S_{175}I$	This study

RKY105-R31/5	*MATa ade2-1 his3-11,15 trp1-1 leu2-3,112 ura3-1 CAN1 arg8::HIS3*	ρ^+*atp6*-$S_{175}D$	This study
RKY105-R33/1	*MATa ade2-1 his3-11,15 trp1-1 leu2-3,112 ura3-1 CAN1 arg8::HIS3*	ρ^+*atp6*-$S_{175}T$	This study
RKY105-R33/4	*MATa ade2-1 his3-11,15 trp1-1 leu2-3,112 ura3-1 CAN1 arg8::HIS3*	ρ^+*atp6*-$I_{171}N$+$S_{175}N$	This study

658

659

660

Table 2. **Intragenic suppressors of the *atp6*-S_{175}N mutation.**

Codon change	Amino acid change	Number
Original mutant		
$TCT_{175}AAT$	$S_{175}N$	-
Intragenic suppressors		
$ATT_{171}TTT$	$I_{171}F$	8
$ATT_{171}AAT$	$I_{171}N$	1
$ATT_{239}TTT$	$I_{239}F$	35
$ATT_{200}ATA$	$I_{200}M$	1
$CCA_{12}TCA$	$P_{12}S$	3
$AAT_{175}GAT$	$N_{175}D$	2
$AAT_{175}AAA$	$N_{175}K$	1
$AAT_{175}ATT$	$N_{175}I$	2
$AAT_{175}ACT$	$N_{175}T$	1
$AAT_{175}AGT$	$N_{175}S$	6

Table 3. Mitochondrial respiration ATP synthesis rates

Strain	Respiration rates nmol $O.min^{-1}.mg^{-1}$				ATP synthesis rate nmol $Pi.min^{-1}.mg^{-1}$		P/O	% ρ^-/ρ^0
	NADH	NADH + ADP	NADH + *CCCP*	*Asc*/*TMPD* + *CCCP*	- *oligo*	+ *oligo*		
WT	410 ± 46	770 ± 40	1400 ± 195	2450 ± 283	828 ± 67	125 ± 21	1.08±0.03	<5%
$S_{175}N$	60 ± 5	60 ± 5	86 ± 5	1064 ± 620	82 ± 9	30 ± 10	1.37±0.04	<35%
$S_{175}N+I_{200}M$	263 ± 58	572 ± 89	763 ± 152	2163 ± 144	729 ± 139	198 ± 64	1.27±0.16	<2%
$S_{175}N+I_{171}F$	368 ± 81	781 ± 94	1422 ± 325	2886 ± 623	796 ± 26	429 ± 29	1.02±0.09	<3%
$S_{175}N+I_{171}N$	122 ± 36	181 ± 74	332 ± 163	1549 ± 284	131 ± 7	74 ± 4	0.72±0.26	<4%
$S_{175}N+P_{12}S$	254 ± 74	424 ± 97	910 ± 308	2603 ± 276	417 ± 34	146 ± 13	0.98±0.14	<6%
$S_{175}N+I_{239}F$	195 ± 51	330 ± 57	660 ± 107	1854 ± 213	347 ± 77	146 ± 30	1.05±0.05	<7%
$S_{175}D$	385 ± 87	674 ± 123	1206 ± 263	2567 ± 186	410 ± 20	197 ± 22	0.61±0.08	<12%
$S_{175}K$	303 ± 49	488 ± 93	745 ± 232	1861 ± 137	360 ± 9	118 ± 11	0.74±0.12	<4%
$S_{175}I$	340 ± 33	738 ± 13	1104 ± 90	2863 ± 142	934 ± 51	184 ± 9	1.27±0.05	<4%
$S_{175}T$	249 ± 62	693 ± 186	772 ± 95	2278 ± 224	965 ± 16	397 ± 28	1.39±0.35	<6%

Mitochondria were isolated from cells grown for 5-6 generations in rich galactose medium (YPGalA) at 28°C. Reaction mixes for assays contained 0.15 mg/mL protein, 4 mM NADH, 150 (for respiration assays) or 750 (for ATP synthesis) µM ADP, 12.5 mM ascorbate (*Asc*),

1.4 mM N,N,N,N,-tetramethyl-p-phenylenediamine (*TMPD*), 4 µM carbonyl cyanide-m-chlorophenyl hydrazone (*CCCP*), 3 µg/mL oligomycin (*oligo*). The values reported are averages of triplicate assays ± standard errors. The percentages of % ρ^-/ρ^o in cultures are indicated.